



## Radiation shielding investigation of PMMA/ZnO doped with nanoparticles of Bi<sub>2</sub>O<sub>3</sub>

Hadeel Kareem Yasser\*, Mohammed J R Aldhuhaibat, Ahmed Jada Farhan

Department of Physics, College of Science, Wasit University, Kut, Iraq.

Email:hadely401@uowasit.edu.iq

6273

### ABSTRACT

This paper studies of amelioration the  $\gamma$ -ray attenuation capacity of the (0.9-x)PMMA+(x)ZnO+0.1Bi<sub>2</sub>O<sub>3</sub> hybrid nanocomposite (where  $x = 0.02, 0.04, 0.06$  and  $0.08$  by weight). The NaI(Tl) detector system and the radioactive source Ra-226, which emits  $\gamma$ -rays with energies of 0.2952, 0.3519, 0.6093, 1.1203 and 1.765 MeV, were used. The attenuation parameters values of  $\mu/\rho$ ,  $\mu$ ,  $A$ ,  $\sigma_a$ ,  $Z_{eff}$ , and  $N_{eff}$  of the proposed hybrid nanocomposite shields as a function of  $\gamma$ -ray energy were calculated. The experimental results of these parameters were compared with those calculated using Phy-X/PSD and XCOM online software. The experimental results of the  $\gamma$ -ray attenuation capacity showed an improvement in all attenuation coefficients when ZnO was added, and the experimental results were in good agreement with the results of theoretical calculations in all the studied hybrid nanocomposites samples.

**Keywords:** the hybrid nanocomposite, linear attenuation coefficient, mass attenuation coefficient,  $Z_{eff}$ ,  $N_{eff}$  and absorbance

DOI Number: 10.14704/nq.2022.20.10.NQ55622

NeuroQuantology 2022; 20(10): 6273-6284

### INTRODUCTION

For more than a decade, the polymer industry and academic research laboratories have been interested in inorganic polymeric nanocomposites of very small size<sup>[1]</sup>. With these materials, it was possible to modify the properties of the polymer by adding specific fillers that are distributed at the nanometer level within the polymeric matrix. They provide the combined advantages of polymer composites, flexibility, ductility and process ability, as well as completely new properties, toughness and high thermal stability of nanostructured materials<sup>[2]</sup>.

Poly methyl methacrylate (PMMA) is a thermoplastic material with high resistivity against abrasion and heat. PMMA material has great thermal, mechanical and radiation shielding properties which can be improved by the addition of colemanite filler. Based on superior structural properties of PMMA material and the additives (colemanite filler), the produced PMMA based polymer composites can be used in different application areas such as the aviation and aerospace field. These new materials have significant advantages such as high durability and high strength. PMMA, commonly Known as "acrylic", has excellent optical clarity, good

abrasion resistance, hardness and stiffness, although the lower mechanical strength and  $\gamma$ -ray shielding ability can be mixed compared to other metal shielding materials with high  $Z$  material to improve mechanical properties and shielding properties. Bismuth (Bi) is being investigated as a potential alternative material in radiation shielding, and plays an important role in the development of the next generation shielding materials with the most desirable properties. Singh et al. conducted a detailed study of  $\gamma$ -rays attenuation and structural properties of the bismuth/glass system<sup>[3]</sup>. During the past decade, nanomaterials with high  $Z$  content in polymer matrices have shown enhanced ability to attenuate and absorb high-energy radiation<sup>[4]</sup>. Radiation shielding is required to protect against penetration of  $\gamma$ -rays because radioactive sources are harmful to human health and sensitive laboratory instruments. There are three parameters for attenuating the intensity of  $\gamma$ -rays: exposure time, distance from the source, and shielding. Among these parameters, the most relevant technique was provided for nuclear radiation protection by shielding with a material of suitable thickness<sup>[5]</sup>. Since radiation is used in large areas and all people must live together with



radiation, shielding is the most important method of radiation protection [6]. The study of the absorption of  $\gamma$ -rays in a shielding material is an important topic in the field of radiation physics. It is potentially useful in developing high-fidelity quasi-experimental constructs. The interaction of high-energy photons with matter is important in radiology, biology, nuclear engineering and space technology. Study of parameters such as mass attenuation coefficient ( $\mu/\rho$ ), linear attenuation coefficient ( $\mu$ ), atomic cross section ( $\sigma_a$ ), electron cross section ( $\sigma_e$ ), effective atomic number ( $Z_{eff}$ ), effective electron density ( $N_{eff}$ ) and absorbency ( $A$ ) is important in understanding the physical properties of composite materials. They are very important in many applied fields such as radiation protection, nuclear medicine, nuclear diagnostics and dosimetry [7].

Many researchers have conducted practical studies of important parameters in radioactive attenuation such as linear and mass attenuation coefficients as well as effective atomic and electronic numbers of many prepared materials to test the possibility of using them in the field of radiation protection such as: ilmenite-magnetite concrete (IM) [8], (Al:Si) and (Al+Na):Si doped ISG

glasses[9]. Other researchers have also conducted theoretical studies to determine the radiative attenuation capacity of different materials such as: P2O5-SiO2-K2O-MgO-CaO-MoO3 glass[10] and bismuth oxide glass [11], Cu2HgI4, Ag2HgI4, and (Cu/Ag/Hg I) Semiconductor Compounds[12] using Phy-X/PSD online software, (Al:Si) and (Al+Na):Si doped ISG glasses using PHY- X/PSD and SRIM software's[9], and some fatty acids (C11H22O2, C12H24O2, C13H26O2, C16H32O2) [13] using the XCOM program, and sodium-doped lead borate glass system (xPbO/(80-x)B2O3/20Na2O) using Phy-x/PSD and WinXCom computer software[14]. The main objective of this study is to experimentally estimate the radiation protection parameters of PMMA/ZnO/Bi2O3 nanocomposite using NaI(Tl) scintillation detector and theoretically using XCOM and Phy-x/PSD online programs in the photon energy range from 0.2952 MeV to 1.765 MeV, and compare the ability of The radiation shielding of this nanocomposite after adding different ratios (2, 4, 6, 8%) of nano-zinc oxide (ZnO) and a fixed ratio 10% of nano-bismuth oxide (Bi2O3) to polymethyl methacrylate in terms of  $\mu/\rho$ ,  $\mu$ ,  $A$ ,  $\sigma_a$ ,  $Z_{eff}$ , and  $N_{eff}$ .

## THEORETICAL BACKGROUND

The coefficient of linear attenuation ( $\mu$ ) is the decrease in the intensity of a photon beam passing through an absorbent material and can be determined by the Lambert-Beer rule [15].

$$I = I_0 e^{-\mu x} \quad \dots\dots\dots (1)$$

Where  $I$  is the intensity at depth ( $x$ ) and  $I_0$  is photon beam intensity before it enters the material.

It is possible to find linear attenuation coefficient experimentally by measure the incoming and outgoing photon beam intensity that passes through the depth  $x$ .

The mass attenuation coefficient can be calculated by ( $\mu/\rho = \mu \times \rho$ ), where  $\rho$  is the density of the sample [16].

The effective atomic number ( $Z_{eff}$ ) which expressed in terms of the atomic cross section  $\sigma_a$  and electronic effective cross section  $\sigma_e$  [17].

$$Z_{eff} = \frac{\sigma_a}{\sigma_e} \quad \dots\dots\dots (2)$$

Where  $\sigma_a$ ,  $\sigma_e$  can be expressed by the following equations,

$$\sigma_a = \frac{(\mu/\rho)_c}{N_A \sum_i \frac{W_i}{A_i}} \quad \dots\dots\dots (3)$$

Where  $W_i$ ,  $A_i$  and  $N_A$  are element fraction weight, element atomic weight and Avagadro's number.

$$\sigma_e = \frac{1}{N_A} \sum_i \frac{f_i A_i}{Z_i} (\mu/\rho)_i \quad \dots\dots\dots (4)$$

Where  $Z_i$ ,  $f_i$  and  $A_i$  are atomic number, mole fraction and atomic weight of the  $i^{th}$  constituent element respectively.

The effective number of electrons per unit mass  $N_{eff}$  can be calculated by the following equation [18].

$$N_{eff} = \frac{(\mu/\rho)_c}{\sigma_e} \quad \dots\dots\dots (5)$$



The absorbency (A) was calculated according to the following equation <sup>[19]</sup>.

$$A = -\log \left( \frac{I}{I_0} \right) \dots\dots\dots (6)$$

Sub. Eq. (1) in Eq. (6)

$$A = -\log (e^{-\mu x}) \dots\dots\dots (7)$$

Where  $\mu$  and X are linear attenuation coefficient and sample thickness respectively.

## MATERIALS AND METHODS

**A. Raw Materials:** Poly methyl methacrylate (PMMA) has been used as a matrix material in this work, which is manufactured by Ottobock Company, Germany. This type of polymer has a special property, as its transmission is approximately 92% transparent; it has very little UV absorption up to 260 nm and high weather capability with high sensitivity. This polymer is used in many applications; it can be used instead of glass, and also can be used in the ultraviolet area, and used as a resistor to electron beam or ion beam in the manufacture of microelectronic chips <sup>[24]</sup>, and two different types of oxides nanoparticles as a reinforcement material. One of them is zinc oxide (ZnO), which manufactured by Xunhou Jiechuang Company for new material technology, with a granular size of (20-30) nanometers were used <sup>[25]</sup>. And the Other is bismuth oxide (Bi<sub>2</sub>O<sub>3</sub>), which were manufactured by Hongwa new material company from China, with a granular size of (20-30) nanometers.

**B. Preparation of PMMA and hybrid nanocomposites:** A clean disposable aluminum container was put on sensitive electronic balance, and the required PMMA was then poured in. 100g of PMMA were mixed with 1g of hardener the content was thoroughly mixed to be ready for specimens casting. The samples were prepared from the hybrid nanocomposites using (2, 4, 6 and 8 wt%) of ZnO and a fixed percentage (10 wt%) of Bi<sub>2</sub>O<sub>3</sub>. The PMMA was mixed with ZnO nanoparticles manufactured by Xunhou Jiechuang with a particle size of (20-30) nm and Bi<sub>2</sub>O<sub>3</sub> nanoparticles of Hongwa with a particle size of (20-30) nm at room temperature manual mixing method according to the proportions identified from Table (1) and Figure (1). They were placed in an oven for 1 hour at 50°C for subsequent treatment, and left for 48 hours before being removed from the molds and left for 7 days prior to any testing to obtain better processing conditions and then stored in vacuum chambers.

TABLE (1). Materials ratios of hybrid nanocomposites.

Sy mbol	Hybrid Shield Components						Density (g/cm <sup>3</sup> )
	Weight fraction (wt%)			Molar fraction (Mol%)			
	C <sub>5</sub> H <sub>8</sub> O <sub>2</sub>	ZnO	Bi <sub>2</sub> O <sub>3</sub>	C <sub>5</sub> H <sub>8</sub> O <sub>2</sub>	ZnO	Bi <sub>2</sub> O <sub>3</sub>	
S1	100	0	0	100	0	0	0.944
S2	88	2	10	95.0230	2.6569	2.3201	1.0532
S3	86	4	10	92.4039	5.2875	2.3086	1.0707
S4	84	6	10	89.8106	7.8921	2.2973	1.0888
S5	82	8	10	87.2427	10.4713	2.2860	1.1075

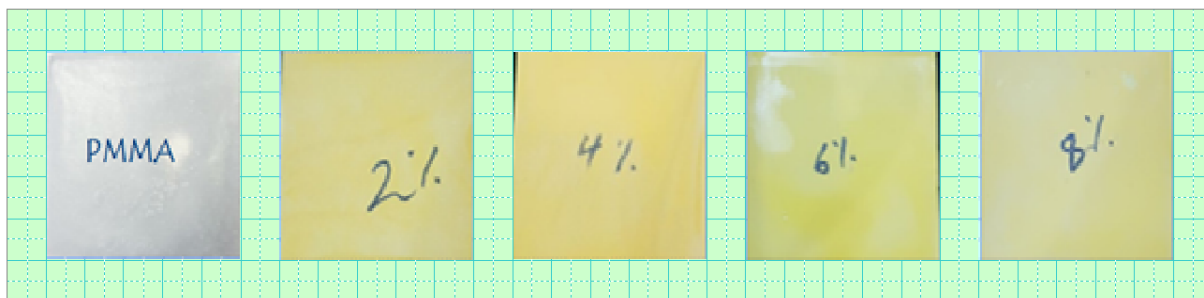


FIGURE 1. The prepared samples



## RADIATION SHIELDING PROPERTIES

Five hybrid nanocomposites samples were prepared for radiological examinations, where the sodium iodide flash detector NaI(Tl) system and the radioactive isotope radium source (Ra-226) were used, which gives a spectrum of  $\gamma$ -rays (0.2952, 0.3520, 0.6093, 1.1203, 1.765 MeV), as the first three energies belong to the radioactive isotope of lead (Pb-214), and the last energies belong to the radioactive isotope Bismuth (Bi-214). The source Ra-226 was used to obtain a spectrum of  $\gamma$ -ray energies, To obtain the narrow beam of  $\gamma$ -rays, lead collimators with a thickness of 1.5cm and a diameter of a central hole of 1.8cm were used, and the distance between the source and the detector was 15 cm. Figure (2) shows the arrangement of the working system.

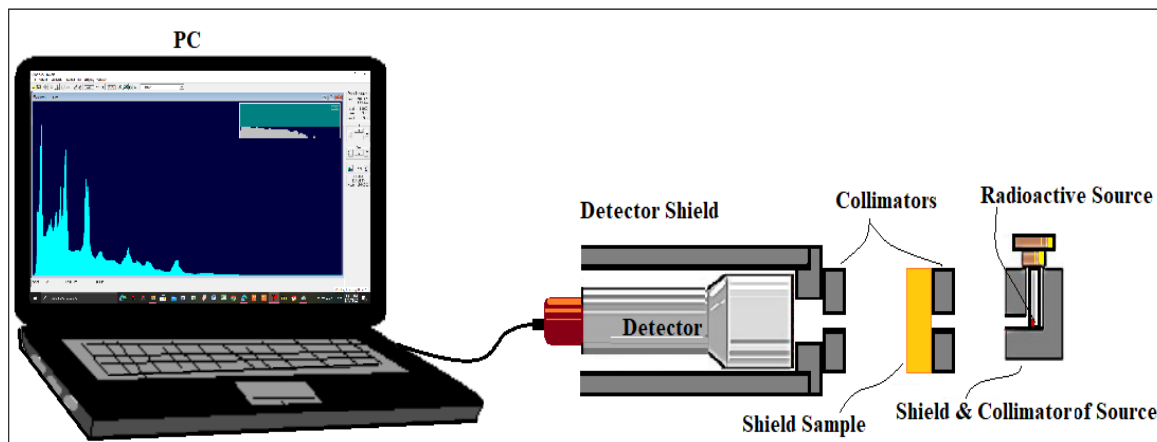


FIGURE 2. Working system arrangement

## RESULTS AND DISCUSSIONS

The results of the experimental calculations of the attenuation parameters of  $\mu/p$ ,  $\mu$ ,  $A$ ,  $\sigma_a$ ,  $Z_{eff}$ , and  $N_{eff}$  for the prepared hybrid nanocomposite as a function of  $\gamma$ -rays energy are shown in Table 2. Phy-X/PSD online program [20] was used at the range of 0.3-2MeV  $\gamma$ -rays energies to obtain theoretical values of limited attenuation parameters, and the XCOM online program [21] was used to obtain theoretical values of  $\mu/p$  for these shields at the  $\gamma$ -rays energies range of 0.2952-2.5 MeV and used to interpolate the other ttenuation parameters.

The obtained attenuation parameters were plotted for the experimentally and theoretically calculated values as a function of  $\gamma$ -ray energy Figure 3, which clearly shows the great concurrence between the experimental values of these parameters with their theoretical values.

In Figures 3-a ,3-b , it can be seen that for all samples, the highest value of  $\mu/p$  and  $\mu$  falls at the lowest energy 0.2952 MeV and its value begins to decrease gradually when the energy increases to reach its lowest value at energy 1.765 MeV, where the highest value of  $\mu/p$  was 0.1453  $\text{cm}^2/\text{g}$  at the lowest energy 0.2952 MeV for sample S2 and the highest value of  $\mu$  was 0.158  $\text{cm}^{-1}$  at lowest energy 0.2952 MeV for sample S5. The reason is that with increasing energy, the probability of photoelectric effect interaction decreases and the probability of Compton scattering and pair production increases, and this is consistent with previous studies [22,23]. The plotted figure of the absorbency coefficient values (Figure 3-c) as a function of  $\gamma$ -ray energy clearly shows that the values of the absorbency ratios decrease with the increase of the  $\gamma$ -ray energy and this behavior is consistent with the behavior of other parameters, where the highest value of the absorbency ratio was 30.87% at energy 0.2952 MeV for sample S5 With a thickness of 4.5 cm, this indicates that increasing the concentrations of additives to the matrix polymer improves the polymer's ability to absorb the intensity of radiation, and this behavior is agrees with [27,28]. The atomic cross-section ( $\sigma_a$ ) values that calculated from eq. (3) were plotted in Figure 3-d and the behavior of  $\sigma_a$  shows a clear decrease with the increase in energy to reach its lowest value at the highest energy (1.765 MeV), where it can be seen that the sample S1 has achieved the minimum values of the atomic cross-sectional area for all the studied energies of  $\gamma$ -rays, the highest value was  $1.88 \times 10^{-24} \text{ cm}^2/\text{g}$  at the lowest energy (0.2952MeV) for sample S5, so that this last sample is



the best among the prepared samples, which supports the previous results in being the best radiation shields, this behavior of the cross-section is consistent with its behavior in previous studies <sup>[13,24]</sup>. The reason can be explained by the dominance of the photoelectric effect in the lower energy range, and also the dependence of the photoelectric effect greatly on the atomic number of the supported material, and one can say that the material containing elements with high atomic number will also have a high atomic cross-section, and this is consistent with previous study <sup>[11]</sup>.

6277

**TABLE (2). Calculated values of radiative attenuation parameters as a function of  $\gamma$ -ray energy for all hybrid nanocomposites.**

Parameter	E (MeV)	Shield Sample				
		S1	S2	S3	S4	S5
$\mu/\rho$ (cm <sup>2</sup> /g)	<b>0.2952</b>	0.1144	0.1453	0.1438	0.1433	0.1427
	<b>0.3519</b>	0.1091	0.1244	0.1261	0.1249	0.1255
	<b>0.6093</b>	0.0869	0.0902	0.0897	0.0891	0.0894
	<b>1.1203</b>	0.0646	0.0665	0.0635	0.0634	0.0650
	<b>1.7650</b>	0.0530	0.0503	0.0504	0.0505	0.0506
$\mu$ (cm <sup>-1</sup> )	<b>0.2952</b>	0.108	0.153	0.154	0.156	0.158
	<b>0.3519</b>	0.103	0.131	0.135	0.136	0.139
	<b>0.6093</b>	0.082	0.095	0.096	0.099	0.097
	<b>1.1203</b>	0.061	0.070	0.068	0.069	0.072
	<b>1.7650</b>	0.050	0.054	0.054	0.055	0.056
$\sigma_a$ $\times 10^{-24}$ (cm <sup>2</sup> /g)	<b>0.2952</b>	1.2678	1.8079	1.8242	1.8527	1.8815
	<b>0.3519</b>	1.2091	1.5479	1.5992	1.6152	1.6552
	<b>0.6093</b>	0.9626	1.1226	1.1372	1.1758	1.1551
	<b>1.1203</b>	0.7161	0.8271	0.8055	0.8195	0.8574
	<b>1.7650</b>	0.5870	0.6263	0.6397	0.6532	0.6669
A%	<b>0.2952</b>	21.1067	29.9012	30.0966	30.4875	30.8783
	<b>0.3519</b>	20.1295	25.6017	26.3834	26.5788	27.1651
	<b>0.6093</b>	16.0255	18.5661	18.7615	19.3478	18.9570
	<b>1.1203</b>	11.9214	13.6803	13.2894	13.4848	14.0711
	<b>1.7650</b>	9.7716	10.3579	10.5534	10.7488	10.9442
$Z_{eff}$	<b>0.2952</b>	3.5595	3.6842	3.7175	3.7755	3.8341
	<b>0.3519</b>	3.6268	3.6855	3.8075	3.8456	3.9409
	<b>0.6093</b>	3.6202	3.8737	3.9242	4.0573	3.9860
	<b>1.1203</b>	3.5821	4.0036	3.8989	3.9665	4.1500
	<b>1.7650</b>	3.7230	3.8610	3.9437	4.0271	4.1113
$N_{eff}$ $\times 10^{23}$ (electron/g)	<b>0.2952</b>	3.2120	2.9603	2.9310	2.9197	2.9072
	<b>0.3519</b>	3.2727	2.9614	3.0019	2.9739	2.9882
	<b>0.6093</b>	3.2668	3.1126	3.0940	3.1377	3.0224
	<b>1.1203</b>	3.2324	3.2170	3.0740	3.0674	3.1467
	<b>1.7650</b>	3.3596	3.1024	3.1093	3.1143	3.1174

The effective atomic number ( $Z_{eff}$ ) and the effective electronic density ( $N_{eff}$ ) which calculated using equations 2 and 5 were plotted in Figure 3-e and 3-f. It appears from figure 3-e that the behavior of  $Z_{eff}$  shows a very slight increase with the increase in  $\gamma$ -ray energy, where the highest value was 4.1501 for sample S5 at energy



1.1203 MeV and this agrees with previous study [13,25]. As for  $N_{eff}$  behavior in figure 3-f, it is linear and close in values with increasing energy. It can be noted that the highest value of this parameter was at the pure polymer, which equals  $3.3596 \times 10^{23}$  electron/g at the highest energy (1.765 MeV), we can conclude from the obtained values showed that the effective electronic density was not significantly affected, and the results were very close to the increase in energy for all samples prepared, and these results were in great agreement with the results of previous studies [26].

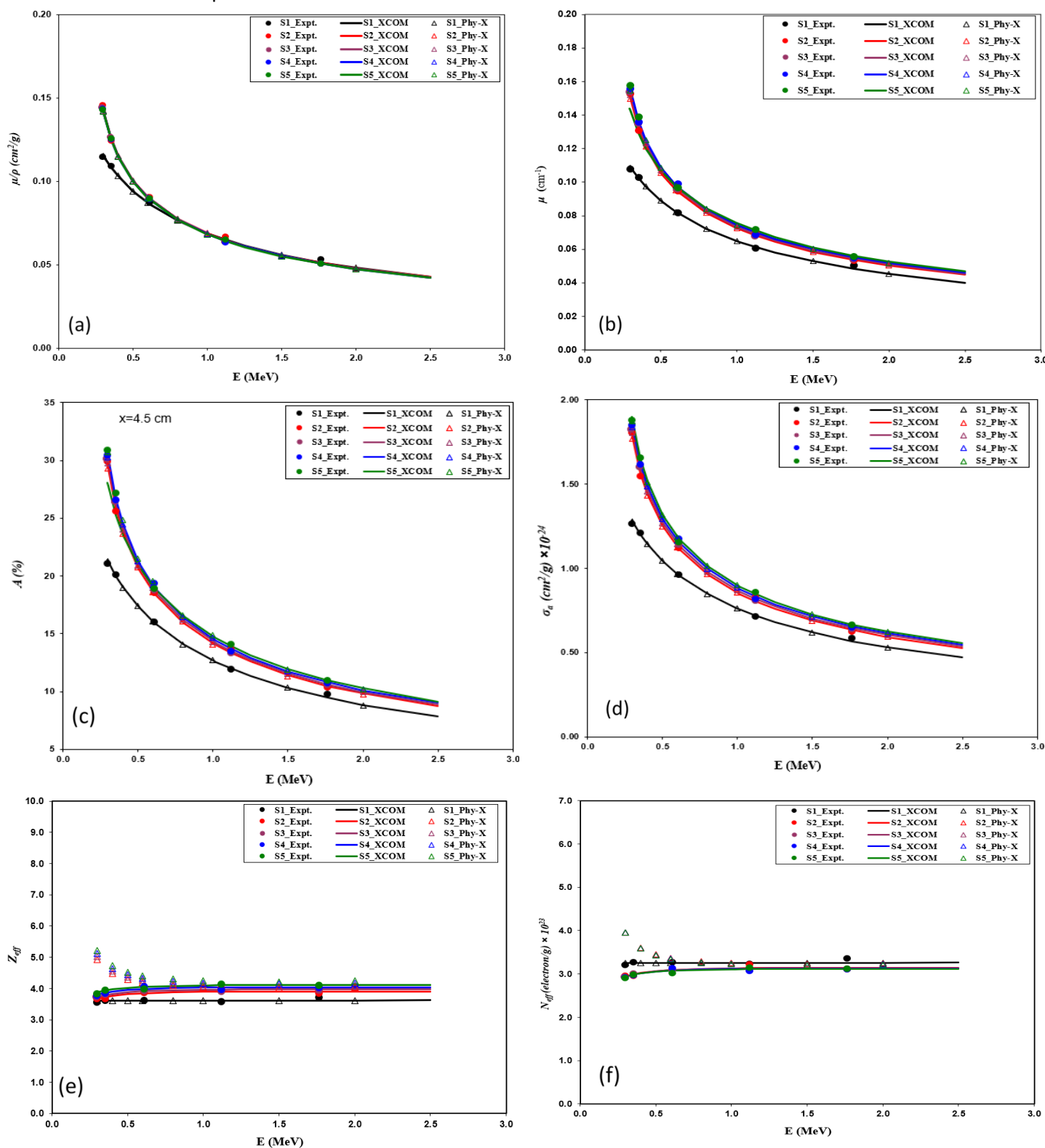


FIGURE 3. Variation  $\mu/\rho$ ,  $\mu$ ,  $A$ ,  $\sigma_a$ ,  $Z_{eff}$  and  $N_{eff}$  values as a function of  $\gamma$ -ray energy.





Figure 4 shows the graph of the attenuation parameter curves ( $\mu/\rho$ ,  $\mu$ ,  $A$ ,  $\sigma_a$ ,  $Z_{eff}$  and  $N_{eff}$ ) against the density of the shield sample at  $\gamma$ -ray energies of 0.2952, 0.3519, 0.6093, 1.1203, and 1.765 MeV. In Figures 4-a , 4-b the results showed that the values of the attenuation factor The mass attenuation coefficient ( $\mu/\rho$ ) and linear attenuation coefficient ( $\mu$ ) increase with increasing density of the shield sample and decreases with increasing  $\gamma$ -rays for all prepared samples, where the highest value of the mass attenuation coefficient was 0.1453  $\text{cm}^2/\text{g}$  at energy 0.2952 MeV for sample S2 with density 1.0532  $\text{g}/\text{cm}^3$  and the highest value of the linear attenuation coefficient  $\mu$  was 0.158  $\text{cm}^{-1}$  at lowest energy 0.2952 MeV with density 1.1075  $\text{g}/\text{cm}^3$  for sample S5 and this is agrees with previous studies [23,29]. Figure 4-c shows that the values of the absorptency ratio increase with increasing sample density and decrease with increasing  $\gamma$ -ray energy for all prepared hybrid samples, and this behavior is consistent with the behavior of the results of the above-mentioned parameters, where the highest value of the absorptency ratio was equal to 30.878% at energy 0.2952 MeV for sample S5 whose density is 1.1075  $\text{g}/\text{cm}^3$ , and this is consistent with the behavior of the results of previous studies [27,28].

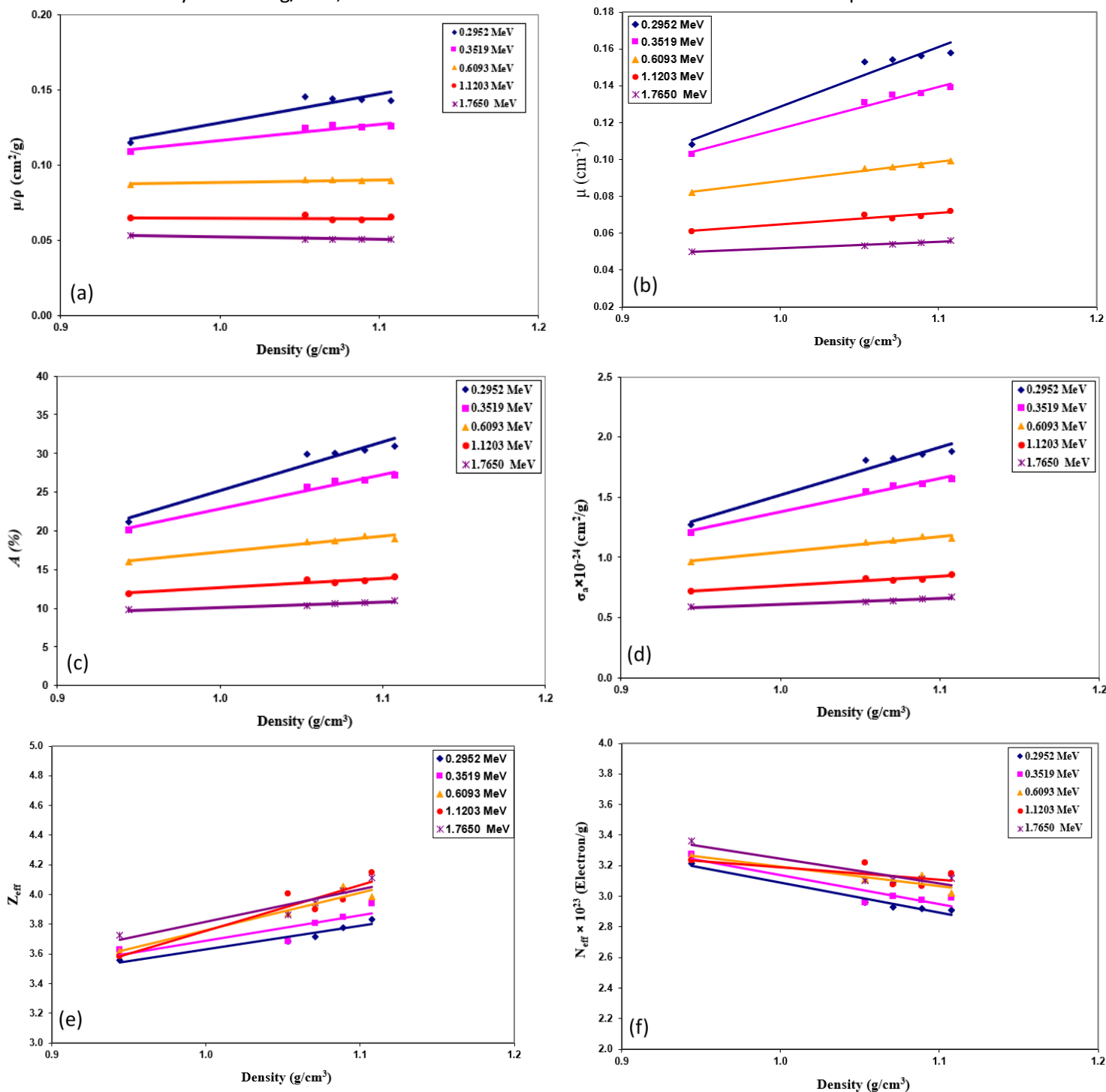


FIGURE 4. Variation  $\mu/\rho$ ,  $\mu$ ,  $A$ ,  $\sigma_a$ ,  $Z_{eff}$  and  $N_{eff}$  values as a function of shield density.



In addition, Figure 4-d shows the values of  $\sigma_a$  versus the density ( $\rho$ ) of the shield sample. This figure shows that  $\sigma_a$  increases with the increase in  $\rho$  of the sample, especially at low energies, for example, the atomic cross-section value of the pure polymer sample S1 is  $1.267 \times 10^{-24}$  cm<sup>2</sup>/g at the lowest energy, but when the density of the sample is increased to 1.1075 g/cm<sup>3</sup> for sample S5, the value of the atomic cross section becomes  $1.8815 \times 10^{-24}$  cm<sup>2</sup>/g, this behavior indicates that increasing the density leads to an increase in the atomic cross section of the hybrid nanocomposite material. Increasing the density improves the shielding properties of the composite material, especially at low  $\gamma$ -ray energies, due to its dependence on the mass attenuation coefficient, which in turn depends on the density of the material. This behavior is consistent with [26]. Figure 4-e shows that  $Z_{eff}$  increases with the increase in  $\rho$  value of the sample, especially at low energies, for example, the value of the effective atomic number of the pure polymer was 3.5595 at the lowest energy, but when the density of the hybrid nanocomposite material was increased to 1.1075g/cm<sup>3</sup>, the value of  $Z_{eff}$  became maximum value (4.1113) at  $\gamma$ -ray energy of 1.765MeV. This behavior indicates that increasing the density leads to an increase in the effective atomic number of the prepared sample. One can conclude that the increasing of sample density improves the shielding properties of the prepared sample due to the increase in the possibilities of major interactions with the increase in the density of the material or in other words with the increase in mass per unit volume, and this behavior is completely consistent with its behavior in the results of previous studies [30]. Figure 4-f shows that the value of  $N_{eff}$  was not affected much with the increase in the density of the composite material and the values were very close, for example, the  $N_{eff}$  value of the pure polymer was equal to  $3.212 \times 10^{23}$  electron/g at the lowest value of the studied  $\gamma$ -ray energy, but when increasing the density of the sample to its highest value (1.1075g/cm<sup>3</sup>), the value of  $N_{eff}$  became equal to  $2.9072 \times 10^{23}$  electron/g, and this behavior indicates that when the density was increased, it did not significantly affect the electronic density of the hybrid composite material [31].

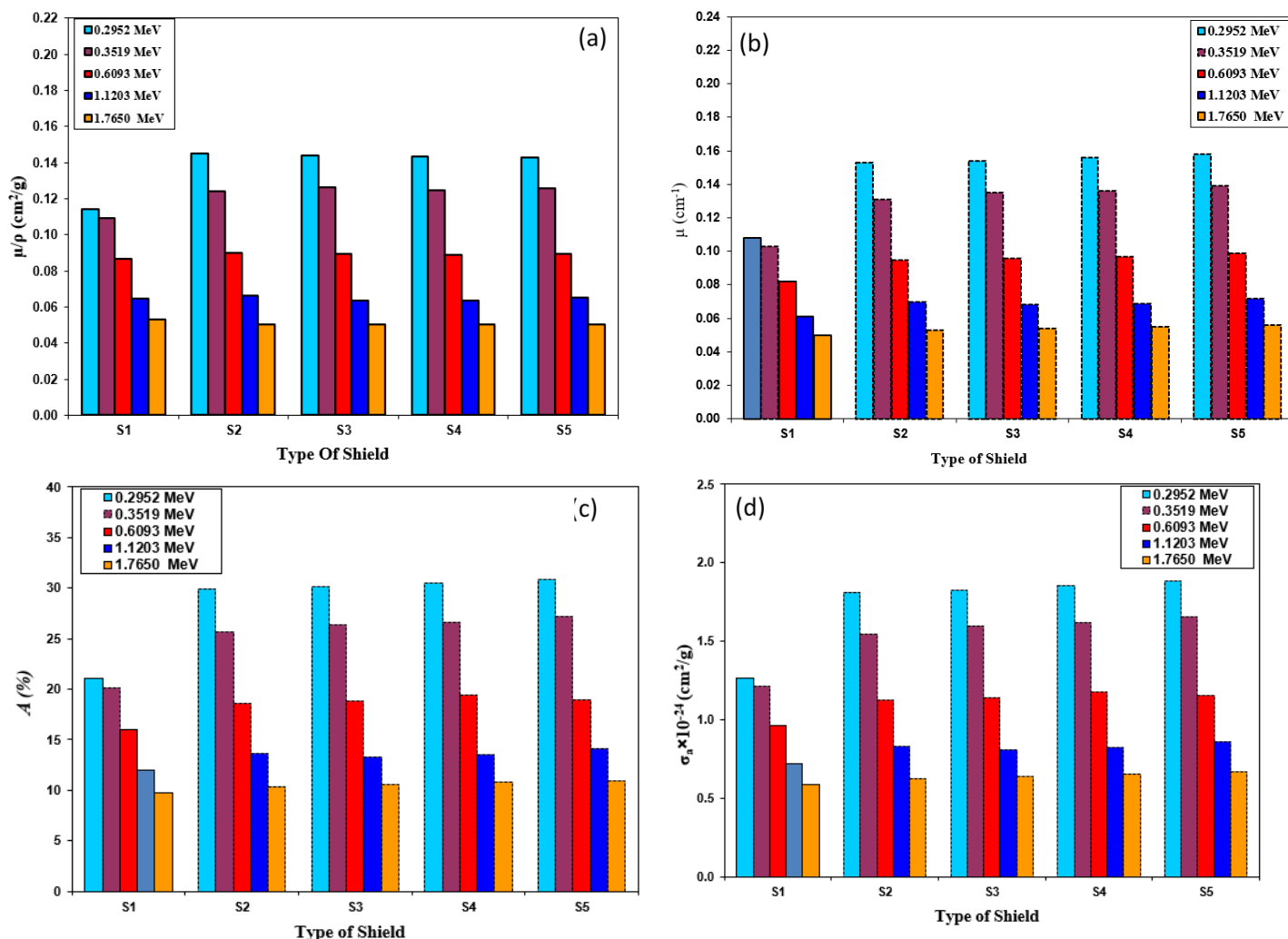
Figure 5 shows the graph of the attenuation parameter curves ( $\mu/\rho$ ,  $\mu$ ,  $\sigma_a$ ,  $Z_{eff}$ ,  $N_{eff}$  and  $A$ ) against the concentrations of the reinforcement materials at  $\gamma$ -ray energies of 0.2952, 0.3520, 0.6093, 1.1203, and 1.765 MeV. It increases with the increase in the concentration of the reinforcement materials (zinc oxide and bismuth oxide), especially at low gamma energies, as it can be seen from the figure that the results are similar in their behavior for all samples prepared at all energies, and this indicates that the increase in the concentration of the reinforcement materials leads to an increase in the coefficient of mass attenuation of the composite material. This significantly improves its radioactive attenuation properties, and the results prove that the maximum value of the mass attenuation coefficient is 0.1453 cm<sup>2</sup>/g for the sample with a concentration of 4% of zinc oxide and 10% of bismuth oxide at a minimum energy of 0.2952 MeV as shown in figure 5-a, and the maximum value of linear attenuation coefficient was at lowest energy 0.2952 MeV for sample S5 as shown in figure 5-b. We can conclude that adding a proportion of zinc oxide and bismuth oxide, respectively, to the pure polymer (polymethyl methacrylate) significantly improves its attenuation properties, and this agrees with previous studies [22,27]. Figure 5-c shows that the values of the absorbcency ratios increase with the increase of the supporting materials and decrease with the increase of the  $\gamma$ -ray energy for all the prepared hybrid samples, and this behavior is consistent with the behavior of the results of the other studied treatments, where the highest value of the absorbcency was equal to 30.878% at energy 0.2952MeV for the sample S5 with The concentration is 8% of zinc oxide and 10% of bismuth oxide. Figure 5-d shows that the atomic cross-section increases with the increase in the concentration of the supporting materials (zinc oxide and bismuth oxide), especially at low  $\gamma$ -ray energies, where the highest value of the atomic cross-section reached  $1.8815 \times 10^{-24}$ cm<sup>2</sup>/g for sample S5 at the lowest energy (0.2952MeV), this behavior is consistent with the results of previous studies [26]. Figure 5 - e This figure shows that the effective atomic number increases with the increase in the concentrations of the reinforcement materials, especially at low energies. From zinc oxide and 10% of bismuth oxide to pure polymer, the value of the effective atomic number became 4.1113, which is the maximum value for it at the same energy. The high percentages of zinc oxide and bismuth oxide, respectively, increase, which in turn increases the possibilities of the main reactions, and then increases the





coefficient of mass and linear attenuation of radiation in the target material, and this is consistent with the behavior of the results of previous studies [13,25]. Figure 5-f, which shows that the effective electronic density was not affected much with the increase in the concentrations of the reinforcement materials and the values were very close, for example, the value of the effective electronic density of the pure polymer was equal to  $3.212 \times 10^{23}$  electron/g at energy 0.2952 MeV, but when increasing the concentration of the reinforcement materials to 8% of zinc oxide and 10% of bismuth oxide, the effective electronic density value became equal to  $2.9072 \times 10^{23}$  electron/g, and this behavior indicates that when the concentration of the reinforcement materials increases, it leads to a relatively slight decrease in the effective electronic density values, and this behavior is completely consistent with his behavior in the results of previous studies [26,31]. This shows us that the reinforcing materials (zinc oxide and bismuth oxide) play an important role in improving the radiative attenuation capacity, and this in turn agrees with the behavior of the results of previous studies [27,28].

6281



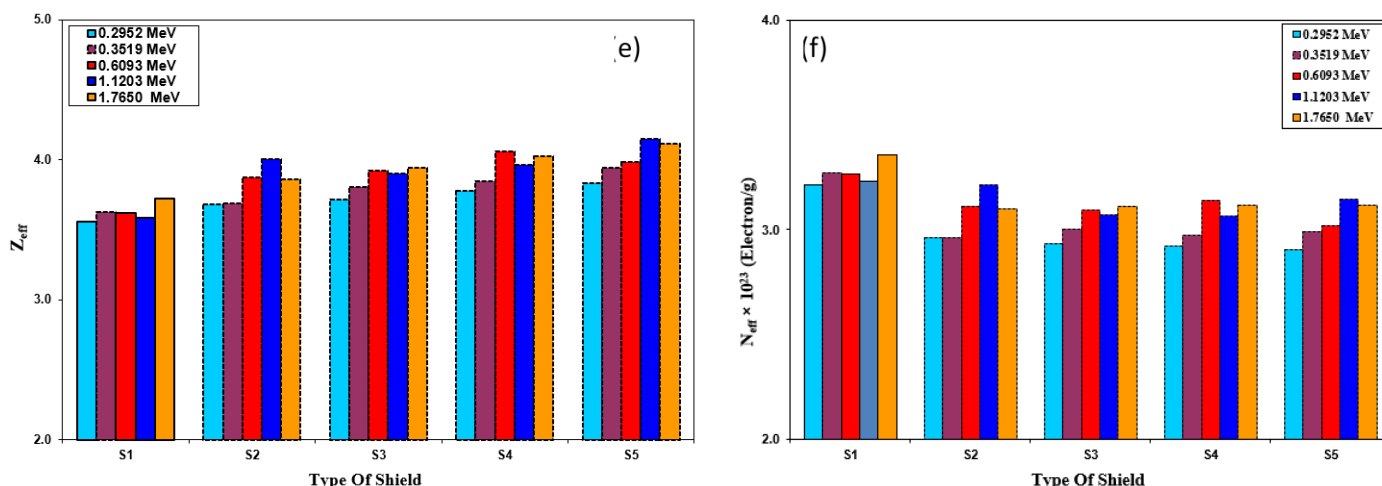


FIGURE 5. Variation  $\mu/\rho$ ,  $\mu$ ,  $A$ ,  $\sigma_a$ ,  $Z_{eff}$  and  $N_{eff}$  values as a function of ZnO concentration.

## CONCLUSIONS

By studying the radioactive attenuation capacity and the structural properties of samples prepared by reinforcement the poly methyl methacrylate polymer (PMMA) with 2%, 4%, 6% by weight of zinc oxide nanopowder (ZnO), and 8% by weight of bismuth oxide nanopowder (Bi2O3) which is described in the general formula of  $(90-x)\%PMMA+10\%Bi_2O_3+xZnO$ , where  $x = 2, 4, 6, 8$  wt%, one can put the most important conclusions that have been reached through the current study, as follows:

1. The values of  $\mu/\rho$  and  $\mu$  decrease with the increase of  $\gamma$ -ray energy for all prepared hybrid nanocomposite samples, as well as the decrease of those parameters with the decrease in both the concentrations of the reinforcement materials in the hybrid nanocomposite samples and the density of those samples.
2. The values of  $A$  increase with the increase in the concentrations of the reinforcement materials and for all the values of  $\gamma$ -ray energies, and it decreases with the increase of  $\gamma$ -ray energies and for all the values of the concentrations of the reinforcement materials.
3. The values of  $\sigma_a$  increased with increasing concentration of ZnO nanopowder and for all  $\gamma$ -rays energies and decreased with increasing  $\gamma$ -rays energy in all prepared hybrid nanocomposite samples.
4. The change in the values of each of  $Z_{eff}$  and  $N_{eff}$  was relatively small, as the values of the first increased and of the latter decreased with an

increase in  $\gamma$ -ray energy in all the prepared hybrid nanocomposite samples. Also, the increase in the concentration of ZnO nanopowder and the density of the prepared samples led to a slightly increase in the values of  $Z_{eff}$  and a slightly decrease in the values of  $N_{eff}$ .

5. The experimental results of this study generally showed a great agreement with the theoretical results studied using the XCOM and Phy-X/PSD online programs.

6. The results of the study proved that the shield S5, represented by the synthetic formula  $82\%PMMA+8\%ZnO+10\%Bi_2O_3$ , achieved the best results in radiation attenuation capacity, making it the best prepared shield for use as a radiation shield.

## REFERENCES

1. Wen, J. and Wilkes, G.L., 1996. Organic/inorganic hybrid network materials by the sol-gel approach. *Chemistry of Materials*, 8(8), pp.1667-1681.
2. Shao, P.L., Mauritz, K.A. and Moore, R.B., 1995. {Perfluorosulfonate ionomer}/[mixed inorganic oxide] nanocomposites via polymer-in situ sol-gel chemistry. *Chemistry of materials*, 7(1), pp.192-200.
3. Kaur, P., Singh, K.J., Thakur, S., Singh, P. and Bajwa, B.S., 2019. Investigation of bismuth borate glass system modified with barium for structural and gamma-ray shielding properties. *Spectrochimica Acta Part A*:



- Molecular and Biomolecular Spectroscopy*, 206, pp.367-377.
4. Udmale, V., Mishra, D., Gadhave, R., Pinjare, D. and Yamgar, R., 2013. Development trends in conductive nano-composites for radiation shielding. *Oriental Journal of Chemistry*, 29(3), p.927.
  5. Jalali, M. and Mohammadi, A., 2008. Gamma ray attenuation coefficient measurement for neutron-absorbent materials. *Radiation Physics and Chemistry*, 77(5), pp.523-527.
  6. E. Al Sarray ,2016."Investigation of Radiation Shielding Properties of Some Composition Materials" MSc. Thesis, Suleyman Demirel University.
  7. Singh, K., Singh, H., Sharma, V., Nathuram, R., Khanna, A., Kumar, R., Bhatti, S.S. and Sahota, H.S., 2002. Gamma-ray attenuation coefficients in bismuth borate glasses. *Nuclear instruments and methods in physics research section B: Beam Interactions with Materials and Atoms*, 194(1), pp.1-6.
  8. Sahadath, H., Mollah, A.S., Kabir, K.A. and Huq, M.F., 2015. Calculation of the different shielding properties of locally developed ilmenite-magnetite (IM) concrete. *Radioprotection*, 50(3), pp.203-207.
  9. KAMIŞLIOĞLU, M., 2021. Investigation of Gama Ray Shielding Properties of the (Al: Si) and (Al+ Na): Si doped International Simple Glasses (ISG) using Phy-X/PSD and SRIM Software's.
  10. Alhuthali, A., Kumar, A., SAYYED, M. and Al-Hadeethi, Y., 2021. INVESTIGATIONS OF GAMMA RAY SHIELDING PROPERTIES OF MoO3 MODIFIED P2O5-SiO2-K2O-MgO-CaO GLASSES. *Digest Journal of Nanomaterials & Biostructures (DJNB)*, 16(1).
  11. Akkurt, I. and Tekin, H.O., 2020. Radiological parameters of bismuth oxide glasses using the Phy-X/PSD software. *Emerging Materials Research*, 9(3), pp.1020-1027.
  12. Zahran, H.Y., Yousef, E.S., Alqahtani, M.S., Reben, M., Algarni, H., Umar, A., Albargi, H.B., Yahia, I.S. and Sabry, N., 2022. Analysis of the Radiation Attenuation Parameters of Cu2HgI4, Ag2HgI4, and (Cu/Ag/Hg I) Semiconductor Compounds. *Crystals*, 12(2), p.276.
  13. Gaikwad, D.K., Pawar, P.P. and Selvam, T.P., 2016. Measurement of attenuation cross-sections of some fatty acids in the energy range 122–1330 keV. *Pramana*, 87(1), pp.1-7.
  14. Taqi, A.H., Salih, A. and Ibrahim, A., 2022. Electromagnetic-Ray Absorption Using B2O3-PbO-Na2O Glass Mixtures as Radiation Protection Shields. *Arab Journal of Nuclear Sciences and Applications*, 55(1), pp.53-61.
  15. Taqi, A.H., Al Nuaimy, Q.A. and Kareem, G.A., 2016. Study of the properties of soil in Kirkuk, IRAQ. *Journal of Radiation Research and Applied Sciences*, 9(3), pp.259-265.
  16. Taqi, A.H. and Khalil, H.J., 2017. An investigation on gamma attenuation of soil and oil-soil samples. *Journal of radiation research and applied sciences*, 10(3), pp.252-261.
  17. Manohara, S.R., Hanagodimath, S.M., Thind, K.S. and Gerward, L., 2008. On the effective atomic number and electron density: a comprehensive set of formulas for all types of materials and energies above 1 keV. *Nuclear Instruments and Methods in Physics Research Section B: Beam Interactions with Materials and Atoms*, 266(18), pp.3906-3912.
  18. Manohara, S.R. and Hanagodimath, S.M., 2007. Studies on effective atomic numbers and electron densities of essential amino acids in the energy range 1 keV–100 GeV. *Nuclear Instruments and Methods in Physics Research Section B: Beam Interactions with Materials and Atoms*, 258(2), pp.321-328.
  19. Libowitzky, E. and Rossman, G.R., 1996. Principles of quantitative absorbance measurements in anisotropic crystals. *Physics and Chemistry of Minerals*, 23(6), pp.319-327.
  20. Şakar, E., Özpolat, Ö.F., Alım, B., Sayyed, M.I. and Kurudirek, M., 2020. Phy-X/PSD: development of a user friendly online software for calculation of parameters relevant to radiation shielding and dosimetry. *Radiation Physics and Chemistry*, 166, p.108496.
  21. Gerward, L., Guilbert, N., Jensen, K.B. and Levring, H., 2004. WinXCom—a program for calculating X-ray attenuation coefficients. *Radiation physics and chemistry*, 71(3-4), pp.653-654.



22. Najam, L.A., Hashim, A.K., Ahmed, H.A. and Hassan, I.M., 2016. Study the attenuation coefficient of granite to use it as shields against gamma ray.
23. Saeed, A., Elbashar, Y.H., Abou El-azm, A.M., El-Okr, M.M., Comsan, M.N.H., Osman, A.M., Abdal-monem, A.M. and El-Sersy, A.R., 2014. Gamma ray attenuation in a developed borate glassy system. *Radiation Physics and Chemistry*, 102, pp.167-170.
24. Sabry, N., Zahran, H.Y., Algarni, H., Umar, A., Albargi, H.B. and Yahia, I.S., 2021. Gamma-ray attenuation, fast neutron removal cross-section and build up factor of Cu<sub>2</sub>MnGe [S, Se, Te] 4 semiconductor compounds: Novel approach. *Radiation Physics and Chemistry*, 179, p.109248.
25. Kucuk, N., Cakir, M. and Isitman, N.A., 2013. Mass attenuation coefficients, effective atomic numbers and effective electron densities for some polymers. *Radiation protection dosimetry*, 153(1), pp.127-134.
26. Hussein, K.I., 2021. Optical and Shielding Parameters of Tellurite Glass with Composition 80TeO<sub>2</sub>-5Nb<sub>2</sub>O<sub>5</sub>-10ZnO-5LiF for Medical Application: Theoretical Investigation. *Int J Opt Photonic Eng*, 6, p.036.
27. Aowd, N.M. and Hussain, H.S., 2015. Absorption coefficient measurement of bremsstrahlung radiation in nano composite. *Engineering and Technology Journal*, 33(7 Part (B) Scientific).
28. Eid, G.A., Kany, A.I., El-Toony, M.M., Bashter, I.I. and Gaber, F.A., 2013. Application of epoxy/Pb<sub>3</sub>O<sub>4</sub> composite for gamma ray shielding. *Arab. J. Nucl. Sci. Appl*, 46(2), pp.226-233.
29. Al-Ghamdi, H., Almuqrin, A.H., Sayyed, M.I. and Kumar, A., 2021. The physical, structural and the gamma ray shielding effectiveness of the novel Li<sub>2</sub>O-K<sub>2</sub>O-B<sub>2</sub>O<sub>3</sub>-TeO<sub>2</sub> glasses. *Results in Physics*, 29, p.104726.
30. Albarzan, B., Hanfi, M.Y., Almuqrin, A.H., Sayyed, M.I., Alsafi, H.M. and Mahmoud, K.A., 2021. The influence of titanium dioxide on silicate-based glasses: An evaluation of the mechanical and radiation shielding properties. *Materials*, 14(12), p.3414.
31. Khedekar, G.H., Pawar, P.P. and Thakare, J.B., 2018. Effective atomic number and mass attenuation coefficient of Vanadium Lead Borate (9V<sub>2</sub>O<sub>5</sub>-71PbO-20B<sub>2</sub>O<sub>3</sub>) glass system within the energy range of 0.122-1.330 MeV.

